BJP British Journal of Pharmacology

DOI:10.1111/bph.12584
www.brjpharmacol.org

RESEARCH PAPER

Targeted inhibition of IL-18 attenuates irinotecan-induced intestinal mucositis in mice

R C P Lima-Júnior[1]*, H C Freitas[2]*, D V T Wong[1], C W S Wanderley[1], L G Nunes[1], L L Leite[1], S P Miranda[1], M H L P Souza[1], G A C Brito[3], P J C Magalhães[1], M M Teixeira[4], F Q Cunha[5] and R A Ribeiro[1,6]

[1]*Nucleus for the Study of Toxicities of the Cancer Treatment, Department of Physiology and Pharmacology, Faculty of Medicine, Federal University of Ceará, Fortaleza, Brazil,* [2]*Department of Oncology, AC Camargo Hospital, São Paulo, Brazil,* [3]*Department of Morphology, Faculty of Medicine, Federal University of Ceará, Fortaleza, Brazil,* [4]*Department of Biochemistry and Immunology, Federal University of Minas Gerais, Belo Horizonte, Brazil,* [5]*Department of Pharmacology, School of Medicine of Ribeirão Preto, University of São Paulo, São Paulo, Brazil, and* [6]*Department of Clinical Oncology, Cancer Institute of Ceará, Fortaleza, Brazil*

Correspondence
Professor Ronaldo Albuquerque Ribeiro, Departamento de Fisiologia e Farmacologia, Faculdade de Medicina, Universidade Federal do Ceará, Rua Cel Nunes de Melo, 1315, Rodolfo Teófilo, 60430-270, Fortaleza, Ceará, Brazil. E-mail: ribeiror21@gmail.com; robertocesar@ufc.br

*These authors contributed equally to the development of this study.

Keywords
cancer chemotherapy toxicity; irinotecan; gut; inflammation; mucositis; IL-18; IL-18 binding protein

Received
12 June 2013
Revised
8 December 2013
Accepted
26 December 2013

BACKGROUND AND PURPOSE
Intestinal mucositis is a common side-effect of irinotecan-based cancer chemotherapy regimens. This mucositis is associated with cytokine activation and NO synthesis. Production of IL-18 is up-regulated in patients suffering from inflammatory bowel disease. Therefore, we have investigated the role of IL-18 in the pathogenesis of irinotecan-induced intestinal mucositis.

EXPERIMENTAL APPROACH
Wild type (WT), IL-18 or caspase-1 knockout mice were treated with either saline or irinotecan (60 mg·kg^{-1} per 4 days, i.p.) or the IL-18 binding protein (IL-18bp, 10 mg·kg^{-1}) before irinotecan. On day 5, diarrhoea was monitored and proximal intestinal strips were obtained for histopathology, *in vitro* gut contractility, myeloperoxidase (MPO) and inducible NOS (iNOS) activity, and detection of IL-18 expression.

KEY RESULTS
Irinotecan induced severe diarrhoea accompanied by intestinal injury (villi shortening and increased crypt depth). Additionally, irinotecan treatment increased MPO and iNOS activity, iNOS immunostaining and IL-18 expression in WT mice compared with saline treatment. The IL-18 production was associated with macrophages. *In vitro*, intestinal smooth muscle strips were hyperresponsive to ACh after irinotecan treatment. Increases in MPO and iNOS activity, intestinal contractility and diarrhoea were prevented in caspase-1 knockout and IL-18 knockout mice, and in IL-18bp-treated WT mice. Furthermore, the Survival of irinotecan-treated mice was increased and iNOS immunoexpression and IL-18 production prevented in IL-18 knockout mice.

CONCLUSIONS AND IMPLICATIONS
Targeting IL-18 function may be a promising therapeutic approach to decreasing the severity of intestinal mucositis during irinotecan treatment regimens.

Abbreviations
ACh, acetyl-choline; IFN-γ, interferon-gamma; IL-1, interleukin-1; IL-12, interleukin-12; IL-15, interleukin-15; IL-18, interleukin 18; IL-18bp, interleukin-18 binding protein; iNOS, inducible form of nitric oxide synthase; KC, keratinocyte-derived chemokine; MPO, myeloperoxidase; NO, nitric oxide; TNF-α, tumour necrosis factor-alpha; WT, wild type

Introduction

Both oral and intestinal mucositis are major dose-limiting side effects of cancer chemotherapy and radiotherapy. Mucositis occurs in approximately 40% of patients on standard dose chemotherapy, and in almost all patients given high-dose chemotherapy and stem cell or bone marrow transplantation, thus affecting over two million people worldwide each year (see Krishna *et al.*, 2011; Gibson *et al.*, 2013). This toxicity significantly affects the quality of life of cancer patients, leading to pain, morbidity, increased supportive care and hospitalization costs, increased frequency of infection, and delays and reductions in chemotherapy (Rubenstein *et al.*, 2004).

Irinotecan, a topoisomerase I inhibitor, is mostly used in the treatment of patients with advanced colorectal cancer, either in combination with one or more agents, such as fluorouracil, oxaliplatin, bevacizumab and cetuximab, or as monotherapy. Irinotecan is usually associated with a high prevalence of grades 3–4 gastrointestinal toxicities, such as mucositis and diarrhoea (Keefe *et al.*, 2007; Hind *et al.*, 2008; Peterson *et al.*, 2011). A number of strategies have been assessed in the management of chemotherapy-related intestinal mucositis, including treatment with sulfasalazine, amifostine, sucralfate, octreotide, hyperbaric oxygen, misoprostol and probiotics (Peterson *et al.*, 2011; Gibson *et al.*, 2013). However, loperamide, an opioid receptor agonist that inhibits peristalsis, remains the main agent used in clinical practice. An understanding of the pathophysiology underlying intestinal mucositis may potentially guide the development of new effective treatment strategies for this inconvenient and prevalent adverse effect of cancer chemotherapy.

We found that irinotecan-induced intestinal damage may be negatively modulated by pentoxifylline and thalidomide administration by inhibiting production of TNF-α, IL-1 and KC (keratinocyte-derived chemokine, the murine IL-8 homologue) (Melo *et al.*, 2008). More recently, we demonstrated that irinotecan-mediated intestinal mucositis was decreased by inhibiting the inducible NOS (iNOS) and could be prevented by the targeted inhibition of cytokines, thus blocking iNOS activation (Lima-Júnior *et al.*, 2012).

IL-18, a member of the IL-1 superfamily, is activated by the intracellular protease caspase-1, generating a biologically active protein with diverse functions, including monocyte and neutrophil chemotaxis, the promotion of T-helper cell differentiation into either T-helper 1 (Th1) or Th2 cells (see Volin and Koch, 2011), and TNF-α and IL-1 activation, which are involved in the pathogenesis of mucositis (Melo *et al.*, 2008). IL-18 function is regulated by the constitutively secreted IL-18 binding protein (IL-18bp), which functions as a natural inhibitor of IL-18 activity and binds to IL-18 with high affinity (Dinarello, 2001).

Chikano *et al.* (2000) suggested that systemic injection of IL-18 in combination with IL-12 induced intestinal mucosal inflammation. In addition, Leach *et al.* (2008) found increased local and systemic IL-18 and IL-18bp production in patients with inflammatory bowel disease, suggesting that this cytokine may contribute to local inflammatory changes. IL-18 production was increased in peripheral blood mononuclear cells obtained from colorectal cancer patients who were treated with irinotecan-based regimens (Xynos *et al.* 2013). However, none of the studies outlined here assessed the contributions of IL-18 to the pathogenesis of intestinal disease.

Here, we have investigated the role of IL-18 in the pathogenesis of irinotecan-induced intestinal mucositis in mice.

Methods

Animals

All animal care and experimental procedures complied with the laboratory animal care and use principles outlined by the National Institutes of Health (NIH publication no. 85–23, revised 1985) and were approved by the local Ethics Committee for Animal Experiments (protocol number 02/04). All studies involving animals are reported in accordance with the ARRIVE guidelines for reporting experiments involving animals (Kilkenny *et al.*, 2010; McGrath *et al.*, 2010). A total of 84 animals were used in the experiments described here.

Caspase-1 knockout mice were generated on a C57BL/6 background from breeding pairs of mice with the targeted disruption of the caspase-1 gene (Jackson Laboratories; Bar Harbor, ME, USA) and back-crossed with C57BL/6 for eight generations. IL-18 knockout mice were similarly generated on BALB/c background from breeding pairs of mice with the targeted disruption of the IL-18 gene (Jackson Laboratories). The genotypes of these mice were confirmed by PCR. The mice were housed in the animal care facility of the School of Medicine of Ribeirão Preto and food and water were available *ad libitum*. Mice were taken to the testing room at least 1 h prior to the experiments. The experiments were performed using male mice (20–25 g). The caspase WT were C57BL/6 and (BALB)/c mice were used as the IL-18 WT when experiments were conducted in IL-18 knockout mice or during the pharmacological modulation of IL-18 function using the IL-18bp.

Induction of experimental intestinal mucositis

Intestinal mucositis in mice was experimentally induced, as described by Ikuno *et al.* (1995), modified for our experimental conditions. Briefly, caspase or IL-18 WT mice were given either saline (3 mL kg^{-1}, i.p.) or irinotecan (60 $mg \cdot kg^{-1}$, i.p., once daily for 4 days). Caspase1 knockout and IL-18 knockout mice were also injected with saline or irinotecan (according to the same protocol). In the additional groups, IL-18 WT animals were treated daily for 4 days with saline (3.5 mL kg^{-1}, i.p.) or IL-18bp (10 $mg \cdot kg^{-1}$, i.p.) 1 h before irinotecan (60 $mg \cdot kg^{-1}$, i.p.) treatment. Diarrhoea was assessed during the treatment period. The animals were killed humanely on the fifth day after the first dose of irinotecan and samples of proximal intestine taken for the measurement of myeloperoxidase (MPO) or iNOS activity, morphometric analyses and evaluation of their contractile properties. A separate set of animals, given the same treatments, were used to follow the survival of the animals, monitored every 24 h for up to 9 days after the administration of the first dose of irinotecan.

Diarrhoea assessment

Diarrhoea was measured using the mean scores, and its severity was quantified according to the procedure described by Kurita *et al.* (2000) as follows: 0 – normal (normal stool or the

absence of stool); 1 – slight (slightly wet and soft stool); 2 – moderate (wet and unformed stool with moderate perianal staining of the coat); and 3 – severe (watery stool with severe perianal staining of the coat).

In vitro *contractility of duodenal strips*

Immediately after killing the animals, strips of duodenal segments (0.5 cm long) were prepared, as described by Lima-Júnior *et al*. (2012). Briefly, the segments were placed in Petri dishes containing modified Tyrode's solution (composition in mM: NaCl = 136.0, KCl = 5.0, $MgCl_2$ = 0.98, $CaCl_2$ = 2.0, NaH_2PO_4 = 0.36, $NaHCO_3$ = 11.9 and glucose = 5.5). After dissection, the luminal content was washed away using a physiological solution. Each segment was then placed in a glass organ bath, filled with 5 mL of Tyrode's solution at 37°C, pH = 7.4 and continuously bubbled with a carbogen (95% O_2/5% CO_2) mixture, and connected to a force transducer (model MLT0201, AD Instruments, Bella Vista, NSW, Australia) under a 1 g resting tension. Longitudinal muscle tension was recorded on a computer-coupled data acquisition system (Chart Pro, Bella Vista, NSW, Australia). After equilibration for 30 min, spontaneous contractions were observed in all of the strips, and two standard contractions of similar magnitude, elicited by 60 mM KCl, were initially recorded as reference contractions for later data normalization. Afterwards, a concentration–response curve for ACh (1×10^{-10} to 1×10^{-4} M) was constructed. The data obtained from this curve were expressed as percentages of the means of the two standard contractions observed with KCl (60 mM). E_{max} was considered to be achieved when an increase in the agonist concentration did not induce a further increase in the contractile response.

Total leukocyte counts

The animals were lightly anaesthetized on the fifth day with 2.5% tribromoethanol (10 mL kg^{-1}, i.p). A blood sample (20 µL) was collected from the retro-orbital plexus of each animal and diluted (1:20) in Turk's solution (380 µL). The leukocyte count per mm^3 of blood was then determined using a Neubauer chamber, as described by Ribeiro *et al*. (1991).

Morphometric analyses

The duodenal samples were fixed in 10% neutral buffered formalin, dehydrated and embedded in paraffin. Sections (5 µm thick) were obtained for haematoxylin–eosin staining (H&E) and for subsequent examinations using light microscopy (100×). For the morphometric analyses, the lengths of the intestinal villi, depths of the Lieberkühn crypts (Software ImageJ 1.4, NIH, Bethesda, MD, USA) and villus/crypt ratios were determined, as previously described by Lima-Júnior *et al*. (2012). Between 5 and 10 villi and crypts were measured per slice.

MPO assay

MPO is an enzyme that is found most abundantly in azurophil neutrophil granules. It was measured in the present study as a neutrophil marker in inflamed tissue by following a previously described colorimetric method (Bradley *et al*., 1982). Briefly, duodenal samples were homogenized in hexadecyltrimethyl-ammonium bromide buffer (50 mg of tissue per mL). The homogenates were then centrifuged at 2000 × *g* for 15 min at 4°C. MPO activity in the resuspended pellets was assayed by measuring the change in absorbance at 450 nm using a reading solution (5 mg of *o*-dianisidine, 15 µL of 1% H_2O_2, 3 mL of phosphate buffer and 27 mL of H_2O). The change in absorbance was recorded and plotted on a standard curve of neutrophil density. The obtained data were expressed as MPO activity (neutrophils per mg of tissue).

Determination of NOS activity

This method is based on the equimolar production of citrulline and NO from arginine, which is mediated by NOS activity. Intestinal samples were homogenized with 0.2 mL of 20 mM HEPES (pH = 7.4) containing 1.25 mM $CaCl_2$, 1 mM DTT and 100 mM tetrahydrobiopterin. Then, 1 mM NADPH and 200 000 cpm of [^{14}C]-arginine (270 µCi $mmol^{-1}$) were added, and the mixture incubated for 15 min at 37°C and centrifuged at 10 000× *g* for 10 min at 4°C. The resulting supernatants were loaded into 2 mL columns of Dowex AG WX-8 (Na+ form 200–400 Mesh, Bio-Rad, Richmond, CA, USA), and were eluted using 3 mL of double-distilled water. [^{14}C]-citrulline levels were then determined using a beta counter. The results were expressed as citrulline production per mg of tissue (Bredt and Snyder, 1989).

Immunohistochemical detection of inducible NOS (iNOS) and nitrotyrosine

Immunohistochemistry for iNOS and nitrotyrosine were performed using the streptavidin-biotin-peroxidase method (Hsu and Raine, 1981) in formalin-fixed, paraffin-embedded tissue sections (5 µm thick) mounted on poly-L-lysine-coated microscope slides. Intestinal cross sections were deparaffinized and rehydrated through xylene and graded alcohols. After antigen retrieval, endogenous peroxidase was blocked (15 min) with 3% (v/v) hydrogen peroxide and washed in PBS. Sections were incubated overnight (4°C) with primary rabbit anti-iNOS or anti-nitrotyrosine antibodies (Santa Cruz Biotechnology, Santa Cruz, CA, USA) diluted 1:400 in PBS plus PBS/BSA. The slides were then incubated with biotinylated goat anti-rabbit antibody (sc-2018 kit, Santa Cruz Biotechnology) diluted 1:400 in PBS/BSA. After washing, the slides were incubated with avidin-biotin-HRP conjugate (sc-2017, ABC Staining System Santa Cruz Biotechnology, Santa Cruz) for 30 min, according to the manufacturer's protocol. iNOS or nitrotyrosine were visualized with the chromogen 3,3′-diaminobenzidine (reference K3468, DAKO liquid diaminobenzidine + substrate, Chromogen System; DAKO North America Inc., Carpinteria, CA, USA). Slides were counterstained with Harry's haematoxylin, dehydrated in a graded alcohol series, cleared in xylene and coverslipped.

Assay of cytokines (IL-18 and IFN-γ) by ELISA

Intestinal samples removed on day 5 from IL-18 knockout and WT mice were used for analysis of cytokines. The intestines were stored at −70°C until required for assay. The collected tissues were homogenized and processed in order to determine their IL-18 and IFN-γ content, by ELISA, as described previously (Melo *et al*., 2008). Briefly, microtiter plates were coated overnight at 4°C with antibody against mouse IL-18 and IFN-γ (2 µg·mL^{-1}). After blocking the plates, the samples and standard at various dilutions were added in duplicate and incubated

at 4°C for 24 h. The plates were washed three times with buffer. After washing the plates, biotinylated sheep polyclonal anti-IL-18 or anti-IFN-γ (diluted 1:1000 with assay buffer 1% BSA), was added to the wells. After further incubation at room temperature for 1 h, the plates were washed and 50 µL of avidin-HRP, diluted 1:5000, were added. The colour reagent *o*-phenylenediamine (50 µL) was added 15 min later and the plates were incubated in the dark at 37°C for 15–20 min. The enzyme reaction was stopped with H_2SO_4 and absorbance was measured at 490 nm. The results are expressed as pg cytokine per mg protein and reported as mean ± SEM.

RNA Isolation and reverse transcriptase reaction

Intestinal samples removed on day 5 from IL-18 knockout and WT mice were used to determine the expression of IL-18 or IFN-γ. A vigorous homogenization of the samples 100 mg·mL^{-1} with 300 mg of 0.1 mm glass beads (BioSpec, Bartlesville, OK, USA) was performed using a MiniBeadBeater (BioSpec). Total RNA isolation was performed using the Aurum™ Total RNA Fatty and Fibrous Tissue Kit (Bio-Rad, Hercules, CA, USA). The yield and quality of total RNA were determined spectrophotometrically using 260 nm and a 260/280 nm ratio, respectively. Total RNA (1µg) from the intestinal samples in a final volume of 20 µL were reverse-transcribed into cDNA in the C1000 Touch™ Termal Cycler system with the iScript™ cDNA synthesis kit from Bio-Rad.

Real-time PCR

All PCRs were analysed by the CFX96 TouchTM real-time PCR detection system instrument from Bio-Rad. Bio-Rad iQTM SYBR® Green Supermix was used in the PCRs for IL-18, IFN-γ and β-actin. Thermal cycling conditions comprised an initial denaturation step at 95°C for 7 min followed by 45 cycles [every cycle begins with a denaturing step (20 s at 95°C), an annealing temperature at 60°C for 20 s and finishes with an extension of 45 s at 72°C]. To ensure the specificity of the PCR product, we conducted a melting curve analysis, in which the reaction temperature was subsequently increased by 0.5°C every 15 s, beginning at 60°C and ending at 95°C and a cooling step at 4°C. All samples were run in duplicate, and each well of PCR contained 20 µL as a final volume, including 1 µL of cDNA, 200 nM gene-specific primers and 10 µL iQTM SYBR Green Supermix. Negative samples were run consisting of no RNA in the reverse transcriptase reaction and no cDNA in the PCR. The threshold cycle (Ct) was compared for the expression of IL-18 and IFN-γ in all tested samples. The relative gene expression was determined using the $2^{-\Delta\Delta Ct}$ (Livak and Schmittgen, 2001) method using β-actin as the housekeeping gene. Primer pairs for mouse IL-18, IFN-γ and β-actin, were as follows:

IL-18	Forward	5′-CAGGCCTGACATCTTCTGCAA-3′
	Reverse	5′-TCTGACATGGCAGCCATTGT-3′
IFN-γ	Forward	5′-TCAAGTGGCATAGATGTGGAAGAA-3′
	Reverse	5′-TGGCTCTGCAGGATTTTCATG-3′
β-actin	Forward	5′-AGAGGGAAATCGTGCGTGAC-3′
	Reverse	5′-CAATAGTGATGACCTGGCCGT-3′

Confocal microscopy

Intestinal samples were obtained and frozen at –70°C in Tissue-Tek® OCT™ compound (Sakura, Torrance, CA, USA); 5 µm sections were cut and blocked with 1% BSA. For three-colour immunostaining, sections were incubated overnight at 4°C with monoclonal rat anti-mouse F4/80 (Caltag Lab, Buckingham, UK) and goat anti-IL18 (Santa Cruz Biotechnology) antibodies, followed by two washes with PBS and incubation with donkey anti-rat Alexa Fluor 488 and donkey anti-goat Texas Red antibodies (Invitrogen, Life Technologies, Grand Island, NY, USA) for 1 h. Sections were then washed twice with PBS, incubated for 5 min with Hoechst 33342 trihydrochloride, trihydrate (Invitrogen, Life Technologies), washed twice with PBS and mounted with antifade mounting medium (Fluoromount-G, SouthernBiotech, Birmingham, AL, USA). Images were acquired using UV laser scanning microscopy confocal microscopy (FLUOVIEW® FV1200, Olympus, Center Valley, PA, USA).

Data analyses

Data are expressed as means ± SEM, with the exception of the diarrhoea assessments, which were reported as the median values (non-parametric data). The data were analysed using either one- or two-way ANOVA followed by Bonferroni's test (parametric data) or the Kruskal–Wallis test followed by Dunn's test (non-parametric data), as appropriate. pD_2 represents the negative logarithm to base 10 of the molar concentration of ACh that produces 50% (EC_{50}) of its maximal possible effect (E_{max}). Such parameters were reported as the means ± SEM. The individual concentration–response curves were analysed using a four-parameter logistic equation $\{y = \min + \max - \min/[1 + (x/EC_{50})^{-\text{Hill slope}}]\}$ for pD_2. Statistical significance was accepted when $P < 0.05$. All data were analysed using GraphPad Prism software version 5.0 (GraphPad Software, Inc., La Jolla, CA, USA).

Materials

Irinotecan hydrochloride (irinotecan, Camptosar®, Pharmacia and Upjohn, Co., Kalamazoo, MI, USA; 100 mg ampoules) and the recombinant IL-18bp (Merck-Serono International, Geneva, Switzerland) were diluted in 0.9% saline.

Results

As shown in Table 1, diarrhoea was significantly higher in the irinotecan-treated caspase-1 and IL-18 WT animals than in the saline-treated WT mice ($P < 0.05$). The IL-18 knockout mice or IL-18bp-treated WT mice treated with irinotecan displayed significant reductions in diarrhoea compared with the irinotecan- treated IL-18 WT group. Despite the mild diarrhoea observed in irinotecan-injected caspase-1 knockout mice (a score of 1.5 on a scale ranging from 1 to 3; Table 1), no significant differences were observed between this group and the irinotecan- treated caspase-1 WT mice. Table 1 also shows that there was significant leukopaenia in the irinotecan-treated mice (which includes caspase-1 WT and knockout mice, IL-18 WT and knockout animals), compared with their respective control groups that received saline.

Representative photomicrographs of duodenal tissue harvested from WT mice and from caspase-1 or IL-18 knockout

Table 1

Diarrhoea assessments and blood leukocyte counts in irinotecan-treated mice

Group	Diarrhoea assessment Scores	Blood leukocyte count Cells per mm^3
Caspase-1 WT + saline	0 (0–0)	10 444 ± 883
Caspase-1 WT + irinotecan	3 (1–3)*	2 900 ± 646*
Caspase-1 knockout + saline	0 (0–0)	10 788 ± 807
Caspase-1 knockout + irinotecan	1.5 (1–3)	1 175 ± 408†
IL-18 WT + saline	0 (0–0)	7 125 ± 883
IL-18 WT + irinotecan	3 (1–3)$^{\infty}$	1 717 ± 291$^{\infty}$
IL-18 WT + IL-18bp + irinotecan	1 (0–2)$^{\#}$	1 983 ± 552$^{\infty}$
IL-18 knockout + saline	0 (0–0)	6 479 ± 1 189
IL-18 knockout + irinotecan	0 (0–2)$^{\#}$	3 281 ± 683$^{\$}$

Parametric and non-parametric data were analysed using ANOVA with Bonferroni's test and Kruskal–Wallis with Dunn's test respectively. Values shown are the means ± SEM (parametric data) or as the medians (minimum–maximum), for non-parametric data.
*$P < 0.05$ versus saline-treated caspase-1 WT control group.
$^{\dagger}P < 0.05$ versus saline-treated caspase-1 knockout group.
$^{\infty}P < 0.05$ versus saline-treated IL-18 WT control group.
$^{\#}P < 0.05$ versus IL-18 WT + irinotecan group.
$^{\$}P < 0.05$ versus saline-injected IL-18 knockout group.

mice are shown in Figures 1 and 2. When administered to WT animals, irinotecan induced prominent reductions in villi height, vacuolization, cell death in crypt regions that leads to the loss of crypt architecture, the disarrangement of epithelial cells (Figures 1B and 2B) and an important neutrophil infiltration (Figure 1E), compared with saline-administered WT mice, which displayed a marked preservation of intestinal structures with no inflammatory infiltration, necrotic or apoptotic cells (Figures 1A and 2A). In irinotecan-injected caspase-1 knockout mice, vacuolated areas in the crypts and apoptotic cells were observed. In addition, some villi areas appeared shortened and flattened when compared with other regions possessing partially preserved villi architecture (Figure 1D); these features clearly differed from those of the tissues of saline-injected caspase-1 knockout mice (Figure 1C). The genetic deletion of IL-18 or pharmacological inhibition of IL-18 (in WT) with IL-18bp contributed to the preservation of the intestinal architecture after irinotecan, exhibiting only a few apoptotic cells and a contiguous epithelial surface (Figure 2D and E, respectively), similar to the architectures in intestinal samples obtained from the saline-treated IL-18 WT or Il-18 knockout mice (Figure 2A and C).

Morphometric analyses revealed that irinotecan treatment in caspase-1 or IL-18 WT mice led to reductions in the villus/crypt ratio compared with the normal WT control animals (Figure 3A–C). In contrast, neither caspase-1 (Figure 3A) nor IL-18 (Figure 3B) knockout mice displayed significant changes to the villus/crypt ratio after irinotecan treatment when compared with saline-injected caspase-1 or IL-18 knockout animals. In addition, tissues from IL-18 WT mice treated with IL-18bp (Figure 3C) showed reduced villus/crypt ratios, in irinotecan-treated samples. However, it is worth noting that the detrimental effects caused by irinotecan were significantly decreased by IL-18bp treatment.

The treatment of caspase-1 or IL-18 WT mice with irinotecan increased MPO (Figure 4, panels A, C and E) and iNOS (Figure 4, panels B, D and F) activity, compared with the control WT animals receiving saline ($P < 0.05$). Such increases in the enzymic activity of MPO and iNOS were not observed in caspase-1 (Figure 4, panels A and B) or IL-18 (Figure 4, panels C and D) knockout mice, compared with their respective control saline-treated knockout animals. In addition, IL-18bp treatment in WT mice (Figure 4, panels E and F) significantly reduced the irinotecan-mediated stimulation of MPO and iNOS activity. Notably, the values for both MPO and iNOS activity, which did not reach statistical difference, were very similar in saline- and irinotecan-treated knockout mice (Figure 4A–D). As shown in panel G, survival was also improved in irinotecan-treated IL-18 knockout mice compared with irinotecan-treated WT mice. Survival was only marginally improved in WT animals treated with IL-18bp ($P = 0.08$ compared with irinotecan-treated WT mice).

Immuno-histological examination of the intestinal samples showed that treatment with irinotecan markedly increased the intensity of iNOS immunostained cells in the lamina propria and in the intestinal epithelial surface of IL-18 WT mice (Figure 5C), compared with saline-injected IL-18 WT animals (Figure 5A). However, immunolabelling for iNOS in the intestinal slices of irinotecan-treated IL-18 knockout mice was attenuated (Figure 5G) when compared with WT animals that received irinotecan (Figure 5C). In addition, the saline-injected IL-18 WT (Figure 5A) and knockout (Figure 5E) mice presented a quite similar, very low intensity of iNOS immunostained cells. It is worth noting that the levels of immunoreactive nitrotyrosine were not affected by irinotecan treatment. Thus the staining was the same in saline-treated IL-18 WT (Figure 5B) or knockout (Figure 5F) mice, and irinotecan-injected IL-18 WT (Figure 5D) or knockout animals (Figure 5H). When the iNOS or nitrotyrosine

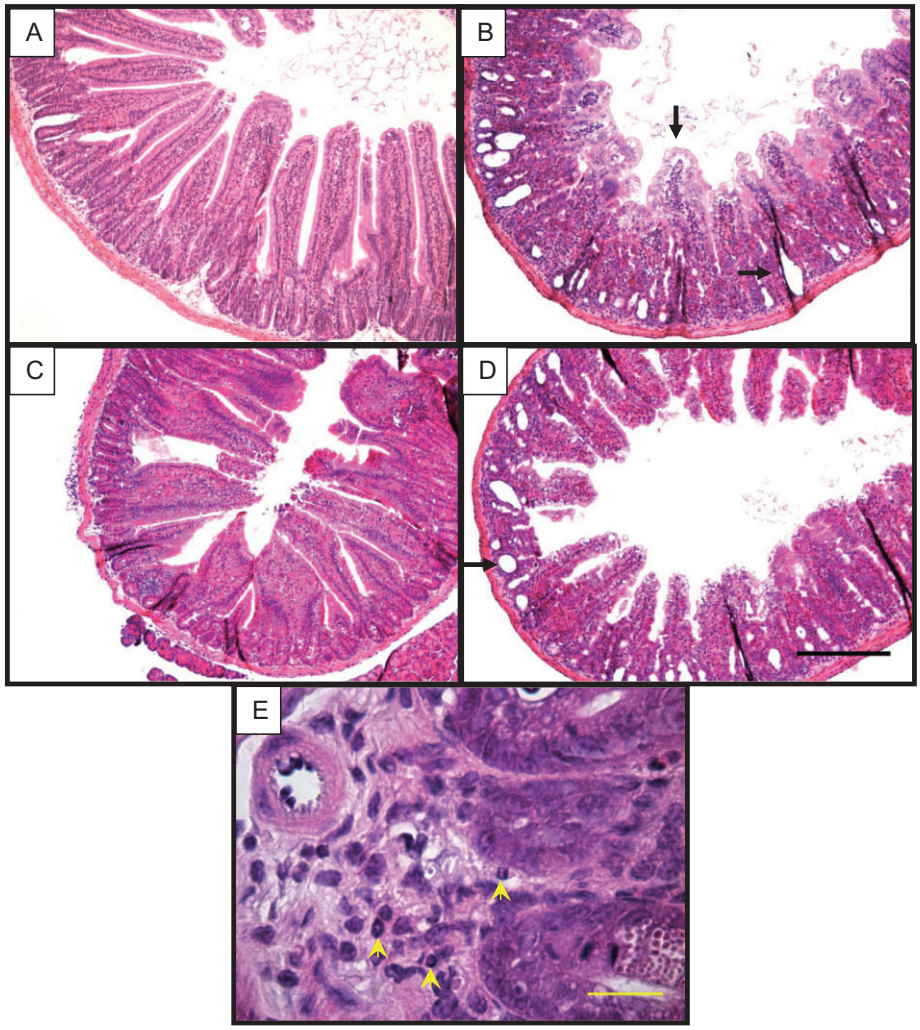

Figure 1

Photomicrographs of duodenal samples taken from WT or caspase-1 knockout (caspase-1$^{-/-}$) mice. Intact intestinal slices from normal WT and caspase-1 knockout mice (A and C, respectively) are presented. Caspase-1 WT animals with irinotecan-induced intestinal mucositis displayed shortened villi (vertical arrows) and the loss of crypt architecture with large vacuolated areas (horizontal arrows) (B). Caspase-1 knockout mice with irinotecan-induced intestinal mucositis displayed partial villi and epithelial cell surface preservation, as well as large vacuolated areas in the crypts (D). Panel E also shows in detail (yellow arrows) the neutrophil infiltrate in irinotecan-treated WT mice. H&E staining (A–D, 100× magnification; E, 1000× magnification). The black and the yellow scale bars represent 200 and 20 μm respectively.

antibodies were replaced by 5% PBS/BSA, no immunostaining was detected (Figure 5I).

Figure 6 shows the expression of IL-18 mRNA (panel A) and IFN-γ (panel B), detected by real-time PCR, and tissue levels of IL-18 (panel C) or IFN-γ (panel D), detected by ELISA, in intestinal samples. Analysis of intestinal tissue from irinotecan- treated IL-18 WT mice showed significantly increased IL-18 mRNA and IL-18 (Figure 6A C, respectively), compared with the WT control group that was given saline. In addition, as expected, neither the saline- nor the irinotecan-injected IL-18 knockout mice expressed IL-18 mRNA or the cytokine protein (Figure 6, panels A and C, respectively). However, IFN-γ expression remained at baseline levels, after irinotecan treatment in the IL-18 WT and in IL-18 knockout mice, compared with saline-treated animals (Figure 6B and D).

Confocal microscopy was performed in order to investigate the involvement of macrophages in the local production of IL-18 during irinotecan-induced mucositis. As shown in Figure 7, the number of macrophages (F4/80 labelled, green cells) was markedly increased in the irinotecan-treated IL-18 WT mice, compared with the saline-injected group. This Figure also shows that IL-18 (red staining) was produced by F4/80^{+} cells (cytoplasmic location) in intestinal slices of the irinotecan-treated animals, but no production of IL-18 was seen in samples from the saline-injected mice (Figure 7).

To assess the contractility of the duodenal samples, concentration–response curves were constructed by adding increasing concentrations of ACh (10^{-10} to 10^{-4} M) to tissues isolated from caspase-1 or IL-18 WT mice and from caspase-1 or IL-18 knockout animals, which had received saline or irinotecan treatment (Figure 8 and Table 2). The data (Figure 8

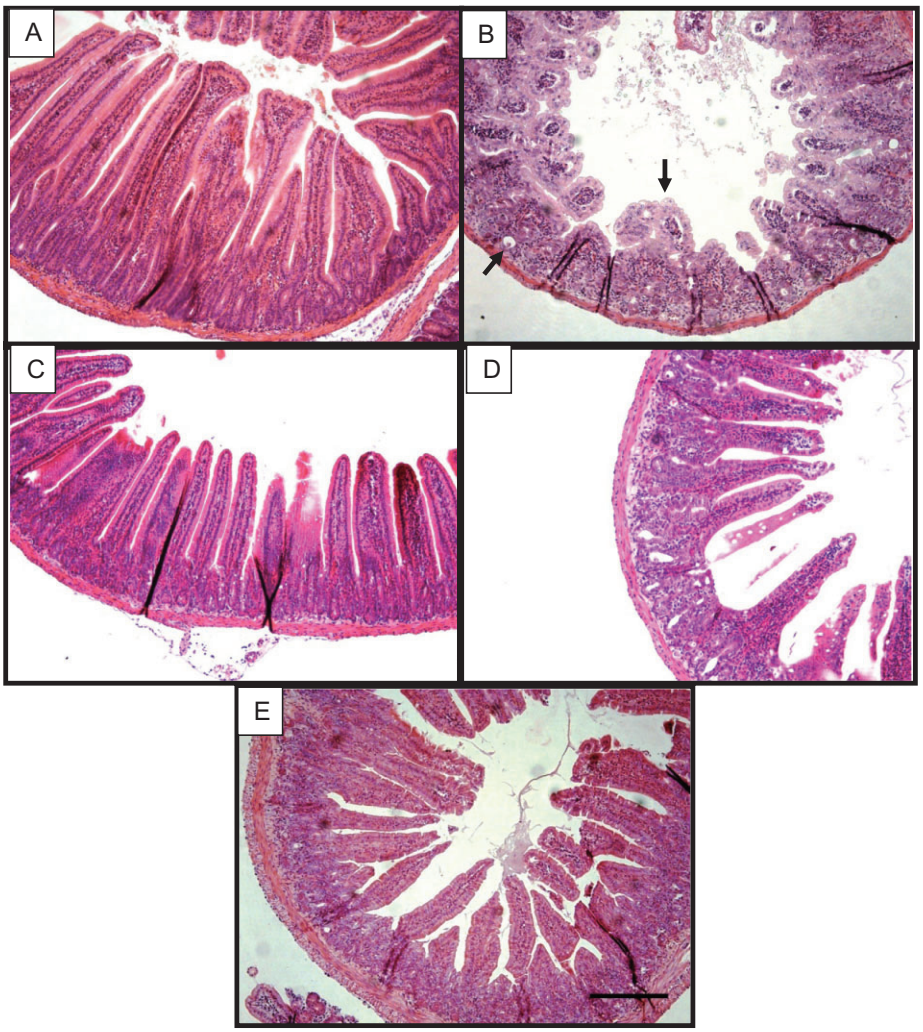

Figure 2

Photomicrographs of duodenal samples collected from WT or IL-18 knockout (IL-18$^{-/-}$) mice and from WT IL-18 mice treated with IL-18bp. Intact intestinal slices from normal IL-18 WT and knockout mice (A and C, respectively) are presented. IL-18 WT animals with irinotecan-induced intestinal mucositis displayed shortened villi (vertical arrows) and the loss of crypt architecture with apoptotic cells (diagonal arrows) (B). IL-18$^{-/-}$ (D) and IL-18bp-treated IL-18 WT (E) mice with irinotecan-induced intestinal mucositis displayed preservation of the crypts, villi and epithelial cell surface. H&E staining (100× magnification). The scale bar represents 200 μm.

and Table 2) showed that intestinal strips from caspase-1 (Figure 8A) or IL-18 (Figure 8B and C) WT mice increased their contractile response to ACh ($P < 0.001$), because these strips achieved higher values for the ACh-induced maximum contractile effect (E_{max}) than tissues obtained from saline-treated WT animals (Figure 8 and Table 2). Such augmented responsiveness to ACh because of irinotecan treatment was absent in both caspase-1 knockout (Figure 8A) and IL-18 knockout (Figure 8B) animals, and in the tissues from IL-18bp-treated WT animals (Figure 8C). The contractile parameters obtained from irinotecan-treated knockout animals were not significantly different from their respective saline controls. It is worth noting that, despite the detected differences in the magnitude of E_{max}, the values for pD_2 remained very close to one another, with no significant differences between them, even in those groups that received irinotecan.

Discussion and conclusions

In the present study, we have demonstrated the involvement of the caspase-1/IL-18 pathway in the predominant irinotecan-induced injury to the gastrointestinal tract – intestinal mucositis. IL-18 was locally produced by macrophages during the intestinal mucositis. In addition, the progression of irinotecan-related intestinal mucositis was prevented by inhibiting caspase-1/IL-18 function, as indicated by improvements in survival, reductions in tissue damage and inflammatory reactions (reduced neutrophil infiltration and inducible NOS immunoexpression), and the amelioration of parameters related to intestinal dysfunction, such as irinotecan-elicited diarrhoea. The caspase-1/IL-18 pathway also appeared to be involved in the increased contractility to ACh exhibited by isolated duodenal strips, obtained from

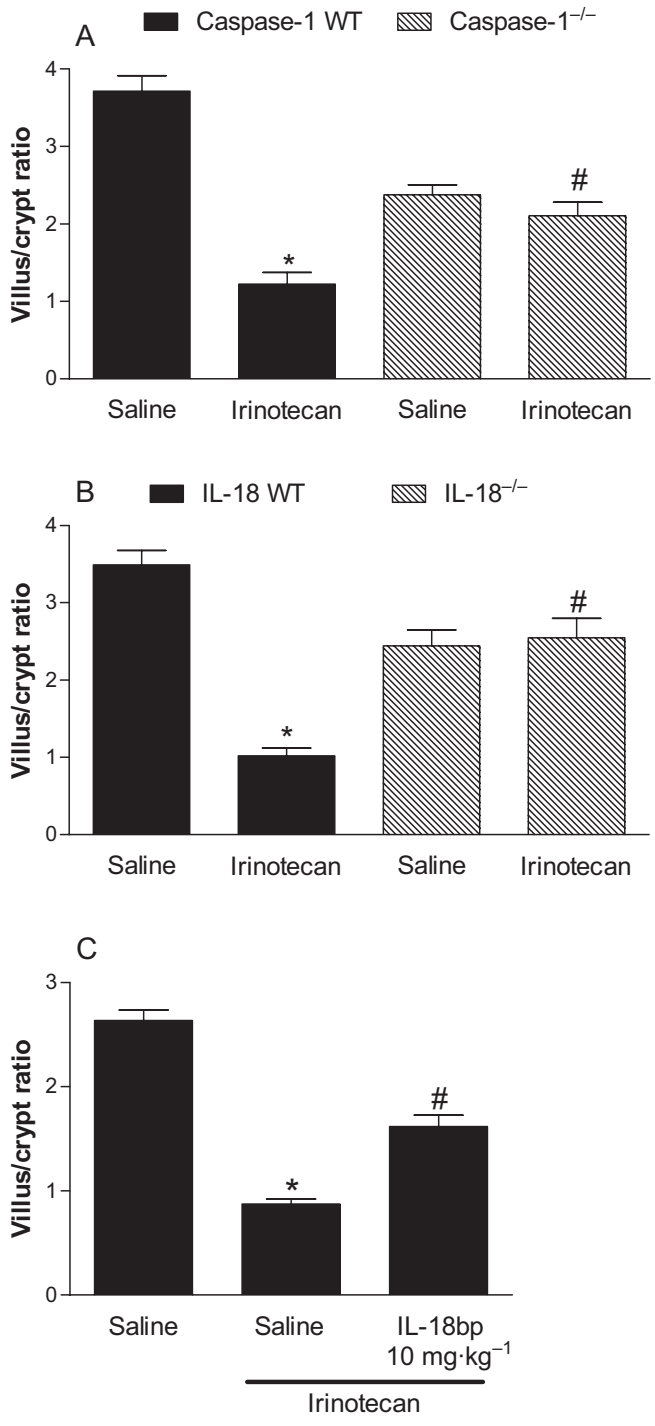

Figure 3

Irinotecan-induced duodenal morphometric alterations are prevented in caspase-1 knockout (caspase-$1^{-/-}$), IL-18 knockout (IL-$18^{-/-}$) and IL-18bp-treated mice. The mice received either saline (3 mL·kg^{-1}) or irinotecan (60 mg·kg^{-1}, i.p) for 4 days and were killed on the fifth day after the first dose. Duodenal segments were taken and processed for histological studies. Morphometric analyses revealed that the treatment of WT mice with irinotecan led to reductions in the villus/crypt ratio compared with normal control animals (panels A–C). In caspase-1 (panel A) or IL-18 (panel B) knockout mice, the villus/crypt ratios were significantly lower than in WT animals, but morphometric alterations were not observed more frequently, even after irinotecan treatment, as revealed by the comparison of these animals with their respective knockout animals that were treated with saline. The treatment of WT mice with IL-18bp significantly blunted the irinotecan-induced reductions in the villus/crypt ratio (C). Data shown are means ± SEM. $^{*}P < 0.05$ versus the WT group that was injected with saline, and $^{\#}P < 0.05$ versus the irinotecan-treated WT group.

irinotecan-treated mice. The results of the present study also indicated that, when administered at a dose previously used by Wyburn *et al*. (2013) just before the first irinotecan injection, IL-18bp protected against all of the intestinal injury-related parameters examined, resulting in significant reductions in inflammatory reactions. It is also important to emphasize that we did not find any strain-related differences in susceptibility to the development of intestinal mucositis between C57BL/6 and BALB/c mice, for any of the parameters studied.

Irinotecan-induced intestinal damage is a well-described phenomenon (Ikuno *et al*., 1995; Gibson and Keefe, 2006; Melo *et al*., 2008; Lima-Júnior *et al*., 2012). A study by Nakao *et al*. (2012) suggested that irinotecan may be attack tight junction proteins, including claudin-1 and occludin, and thus disrupt the intestinal epithelial barrier, an event that can potentially induce bacterial translocation and diarrhoea. Under inflammatory conditions, the presence of apoptotic foci and altered tight junction structures is believed to contribute to the development of diarrhoea by favouring the leakage of absorbed fluids across the tight junctions into the lumen, creating a condition that appears to be worsened by augmented intestinal contractility (see Wenzl, 2012). As described in our study, irinotecan induced marked intestinal damage that was accompanied by the loss of normal architecture and an increased number of apoptotic cells in the crypt, together with increased IL-18 mRNA expression and IL-18 production. This damage was significantly decreased in IL-18 knockout and IL-18bp-treated mice, as demonstrated by the villus/crypt ratio and also the expression of IL-18 was, as expected, abolished in IL-18 knockout mice. However, the knockout of caspase-1 did not prevent irinotecan-associated intestinal damage, and these animals displayed large vacuolated areas and significant diarrhoeal events.

The activation of caspase-1 in the inflammasome is responsible for the proteolytic processing of the immature forms of IL-1β and IL-18, two very powerful proinflammatory cytokines with pleiotropic activities (see Sahoo *et al*., 2011). One likely explanation for the lessened protective effect provided by the genetic deletion of caspase-1 against intestinal damage is that caspase-1 only partly controls IL-18 activation. There are known to be other, inflammasome-independent, mechanisms for the processing and activation of cytokines (van de Veerdonk *et al*., 2011), which may account for the less effective protection against mucositis in caspase-1 knockout mice for some of the parameters studied (such as diarrhoea and intestinal architecture). However, much greater protection against the inflammatory and functional aspects of mucositis was observed in each of the modulating mechanisms investigated, including MPO and iNOS activity,

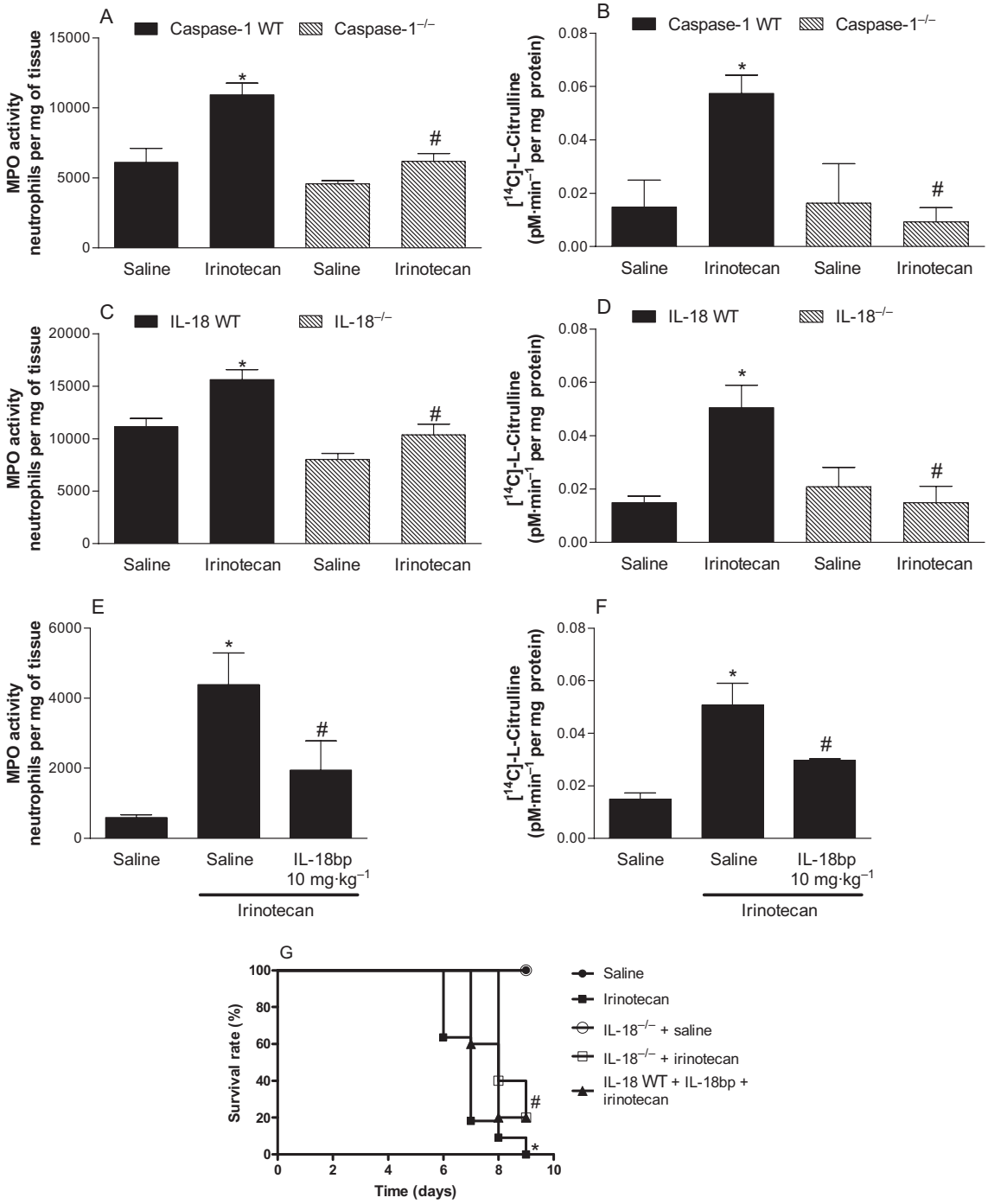

Figure 4

Inflammatory reactions are prevented in caspase-1 knockout (caspase-1$^{-/-}$), IL-18 knockout (IL-18$^{-/-}$) and IL-18bp-treated IL-18 WT mice. The mice were injected with either saline (3 mL kg^{-1}) or irinotecan (60 mg·kg^{-1}, i.p) for 4 days and were killed on the fifth day after the first dose. Samples of duodenum was collected and processed for use in MPO and NOS assays. Irinotecan treatment in WT mice increased MPO (panels A, C and E) and iNOS (panels B, D and F) activity compared with normal control animals. Caspase-1 (panels A and B) and IL-18 (panels C and D) knockout or pharmacological modulation with IL-18bp (panels E and F) significantly prevented these responses compared with irinotecan-injected WT animals. Survival was also improved in irinotecan-injected IL-18 knockout mice (panel G) compared with irinotecan-injected IL-18 WT animals. The values are expressed as the means ± SEM. *$P < 0.05$ versus the WT group that was injected with saline, and $^{\#}P < 0.05$ versus the irinotecan-treated WT group.

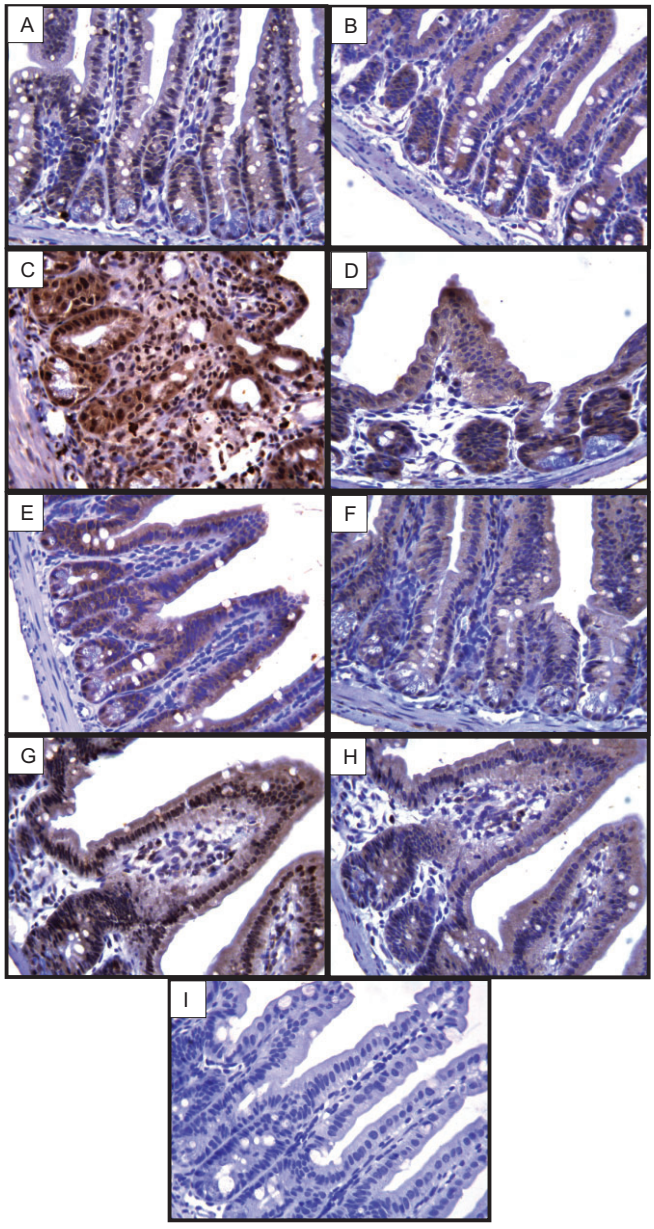

Figure 5

iNOS immunoexpression is prevented in IL-18 knockout (IL-18$^{-/-}$) mice. The mice were injected with either saline (3 mL·kg^{-1}) or irinotecan (60 mg·kg^{-1}, i.p) for 4 days and were euthanized on the fifth day after the first dose was administered. A portion of the intestine was collected and processed for immunohistochemistry to iNOS and nitrotyrosine. Irinotecan injection in WT mice showed intense immunoexpression for iNOS (panel C) versus saline-injected WT mice (panel A). However, IL-18 knockout mice that received irinotecan markedly presented a reduced the number of iNOS labelled cells (panel G), similar to saline-injected IL-18 knockout animals (panel E), when compared with irinotecan-injected IL-18 WT mice (panel C). Nitrotyrosine immunoexpression did not vary in spite of the injection of irinotecan (panels B and D represent saline and irinotecan-injected WT mice; panels F and H represent saline and irinotecan-injected knockout mice). Negative control represents a sample of the intestine where the iNOS or nitrotyrosine antibodies were replaced by 5% PBS/BSA and no immunostaining was detected (panel I). Representative photomicrographs are shown: 400 × magnification.

diarrhoea and intestinal hyperresponsiveness to ACh, in both IL-18 knockout and WT mice treated with IL-18bp.

In a previous paper, we demonstrated that cytokines were required for iNOS activation and NO synthesis (Lima-Júnior *et al.*, 2012) and NO has been associated with the gastrointestinal toxicity of several anticancer chemotherapy agents (Leitão *et al.*, 2007; 2011; Lima-Júnior *et al.*, 2012). In the current study, IL-18 signalling was critically involved in the increased iNOS activity, as iNOS immunoexpression was markedly increased in WT mice and, additionally, reduced in IL-18 knockout mice. Taken together, these findings confirm IL-18 as an important regulator of NO activation.

Once formed, NO can rapidly react with superoxide radicals to form peroxynitrite, a powerful oxidizing agent that contributes to the nitration of tyrosine residues in proteins, which partly explains the tissue toxicity following excessive NO formation (Alvarez and Radi, 2003). Nitrotyrosine is recognized as a marker of the contribution of NO to oxidative damage to proteins (Alvarez and Radi, 2003) but in our study, we did not observe any increase in nitrotyrosine formation, associated with irinotecan treatment. However, as peroxynitrite also reacts with acidic amino acids, including cysteine and methionine, and with prosthetic groups, particularly transition metal centres (see Alvarez and Radi, 2003), we cannot totally exclude a role for this free radical in the intestinal damage induced by irinotecan.

Several studies have contributed to the current state of knowledge regarding the role of IL-18 in tissue injury (Verri *et al.*, 2007; Matsunaga *et al.*, 2011; Wyburn *et al.*, 2013). Wyburn *et al.* (2013) recently demonstrated that doxorubicin, an anticancer agent that inhibits topoisomerase II, induced nephrotoxicity in an IL-18-dependent manner. These authors also showed that IL-18 neutralization with IL-18bp was protective, by reducing the mRNA levels of pro-inflammatory cytokines, chemokines and iNOS, suggesting that IL-18 may coordinate local effector mechanisms of renal injury through a range of macrophage-mediated and Th1- and Th17-type responses (Wyburn *et al.*, 2013). Moreover, Matsunaga *et al.* (2011) also found that IL-18 was involved in the pathophysiology of the proinflammatory response in colonic inflammation under psychologically stressful conditions, using IL-18 knockout mice and an anti-IL-18 antibody. Furthermore, Verri *et al.* (2007) proposed that IL-18 activation signalled through CXCL2, CCL3, TNF-α and LTB_4 to recruit neutrophils to inflammatory foci during inflammatory autoimmune diseases. We believe that, in our study, IL-18 is likely to have orchestrated similar chemokine cascades and that its inhibition consequently prevented the activation of other proinflammatory mediators and the intestinal damage.

Additionally, together with IL-12, IL-18 participates in the Th1 paradigm, mainly because of its ability to induce IFN-γ, either with IL-12 or IL-15. Without IL-12 or IL-15, IL-18 does not induce IFN-γ, playing a role in Th2 responses (Dinarello *et al.*, 2013). Interestingly, in our study, IFN-γ was not expressed, which might be a clear indication that Th2 responses were elicited in our model. Another likely suggestion for the low level of IFN-γ production in our animal model is that the time, the fifth day, chosen for the collection of the intestinal samples was too early for the tissue expression of that cytokine. As IFN-γ is a key regulator of the adaptive Th1 immune response, it is possible that the onset of the

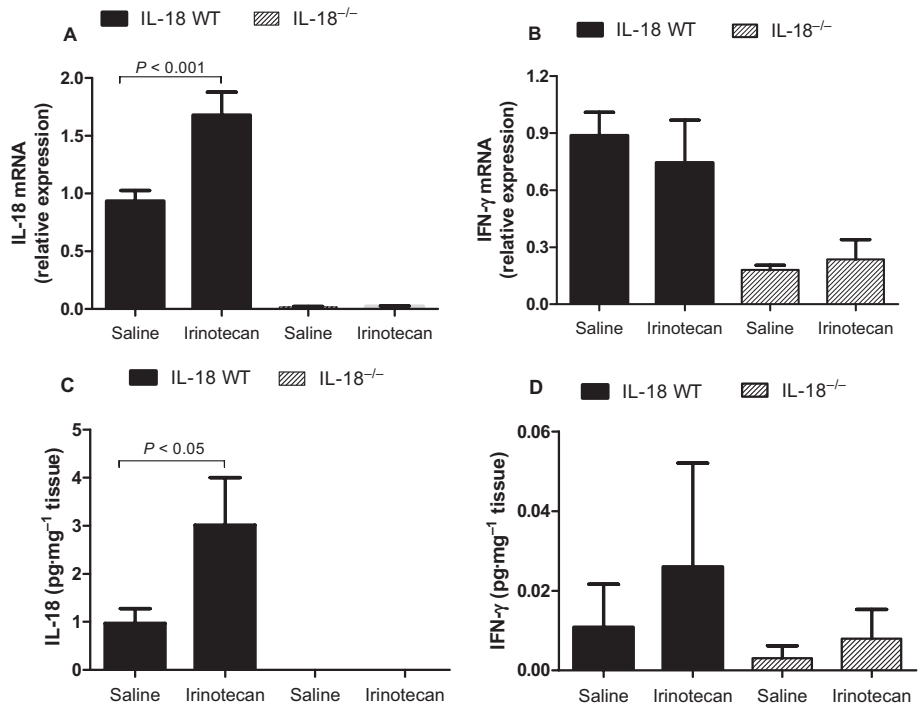

Figure 6

Irinotecan induces IL-18 expression. The mice were injected with either saline (3 mL·kg^{-1}) or irinotecan (60 mg·kg^{-1}, i.p) for 4 days and were killed on the fifth day after the first dose was administered. Samples of duodenum were collected and processed for quantitative PCR (panels A and B) and ELISA (panels C and D). IL-18 mRNA was highly expressed (panel A) and IL-18 production levels were increased (panel C) in the irinotecan-injected IL-18 WT mice ($P < 0.001$) when compared with WT animals which received saline (panels A and C). In contrast, saline- or irinotecan-treated IL-18 knockout (IL-18$^{-/-}$) mice showed no IL-18 expression ($P > 0.05$, panels A and C). IFN-γ mRNA and the IFN-γ production levels were not altered during irinotecan administration and no statistical difference was found between groups ($P > 0.05$, panels B and D).

intestinal injury, i.e. the early phases of the mucositis, would be partly driven by the innate immune response. Therefore, tissue collection on day five of the experimental model of mucositis may represent a transition between the innate and the adaptive immune responses. However, the role of the adaptive immune response in the pathogenesis of intestinal mucositis should be investigated.

A relevant question is whether IL-18 could be locally produced and which cells would be involved. Although our confocal microscopy studies identified macrophages in the lamina propria as a source of IL-18, this does not exclude the participation of other cells in the production of IL-18, including endothelial cells, keratinocytes and intestinal epithelial cells throughout the gastrointestinal tract (see Dinarello *et al.*, 2013).

Inflammation is characterized by early neutrophil influx to the site of inflammation, and the ensuing chronicity of inflammation is sustained by Th1-like immune responses (Verri *et al.*, 2007). Several studies have indicated that cytokine modulation contributed to reduced neutrophil accumulation (as detected by reductions in MPO activity) in the gut during mucositis, thereby reducing tissue damage (Kurita *et al.*, 2000; Melo *et al.*, 2008; Lima-Júnior *et al.*, 2012; Soares *et al.*, 2013). Here, we found that IL-18 or caspase-1 knockout mice or IL-18bp treatment clearly decreased neutrophil influx in the intestine, but the role of neutrophils in the pathogenesis of intestinal mucositis merits further study.

The inflammatory reaction during mucositis was previously described to partially modify the contractile behaviour of isolated intestinal strips in response to cholinergic agonists (Lima-Júnior *et al.*, 2012), which may be correlated with the visceral cramps that are experienced clinically by patients. The results of the present study also show that the genetic deletion of caspase-1 or IL-18, or the pharmacological inhibition of IL-18 prevented intestinal hyperresponsiveness to ACh *in vitro*, shown by the lowering of the maximum effect response (E_{max}) of isolated intestinal strips to ACh, towards the levels observed in control tissues. However, the pharmacological potency of ACh was not affected because the pD_2 values were not significantly different in tissues obtained from animals after irinotecan treatment. These findings strongly support the idea that the population of muscarinic cholinergic receptors is maintained during the establishment of intestinal mucositis, while the ability of ACh to induce contraction via these receptors appears to be augmented.

A 'cholinergic syndrome', associated with high-dose irinotecan administration, has been observed 1 h after dosing and consists of lacrimation, miosis, increased salivation, diaphoresis, flushing, rhinitis and intestinal hyperperistalsis, which usually leads to early onset diarrhoea (see Hyatt *et al.*, 2005). In clinical practice, this cholinergic syndrome is usually prevented by atropine, a muscarinic receptor antagonist. Hyatt *et al.* (2005) hypothesized that atropine may interact with, and inhibit, AChE as irinotecan and its

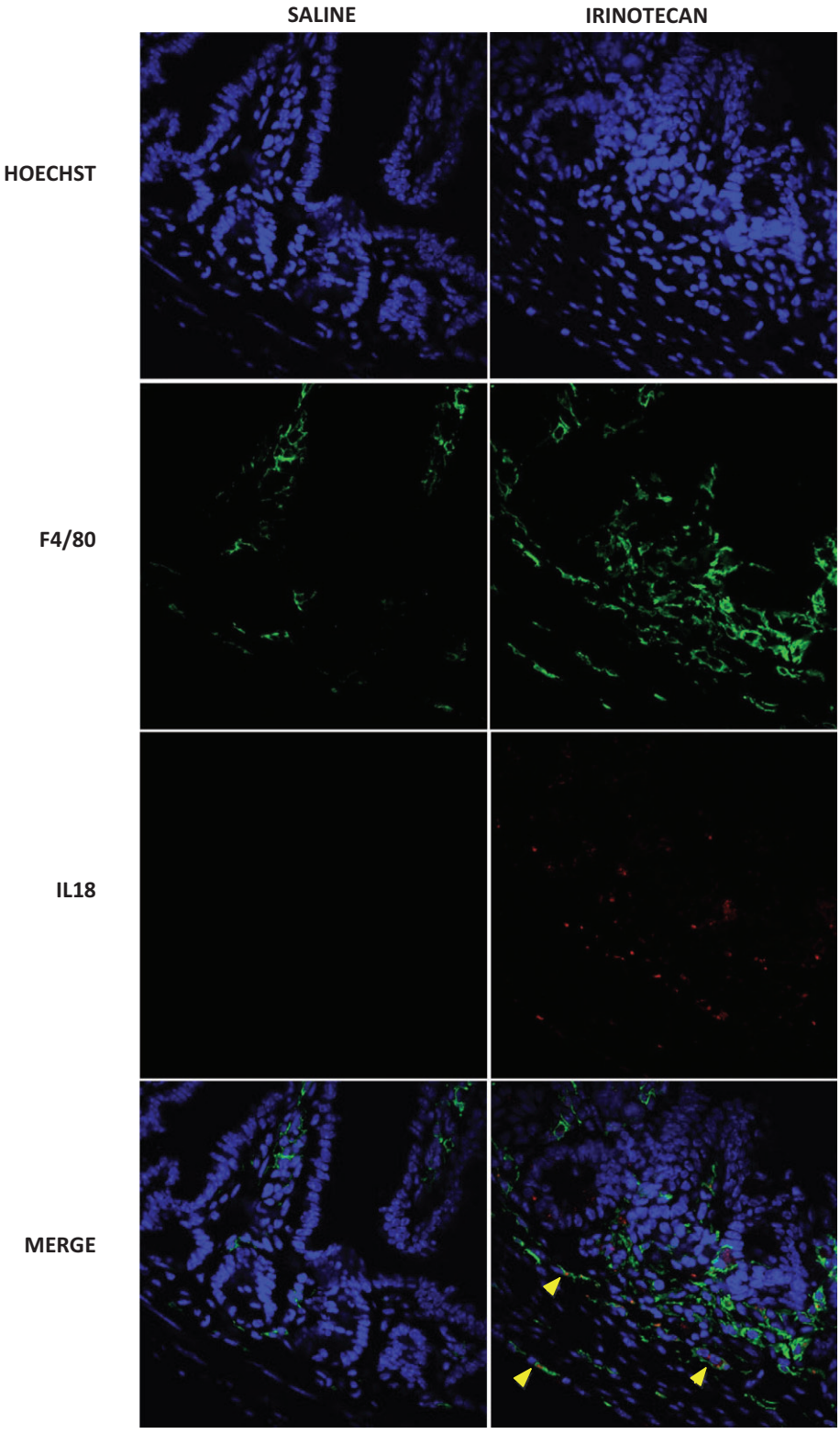

Figure 7

Macrophages are an important source of IL-18 during irinotecan-induced intestinal mucositis. The IL-18 WT mice were injected with either saline (3 mL·kg^{-1}) or irinotecan (60 mg·kg^{-1}, i.p) for 4 days and were killed on the fifth day after the first dose was administered. Duodenal samples were collected and processed for confocal microscopy. Irinotecan injection increased the number of F4/80 labelled cells (macrophages, green cells) when compared with saline-treated mice. In addition, it also shown that the IL-18 (red staining) is produced by F4/80^{+} cells (green cells) in irinotecan group (cytoplasmic location), but no IL-18 fluorescence was observed in intestinal slices of the saline group. Representative photomicrographs are shown. Double-positive cells are indicated by yellow arrowheads (500 × magnification).

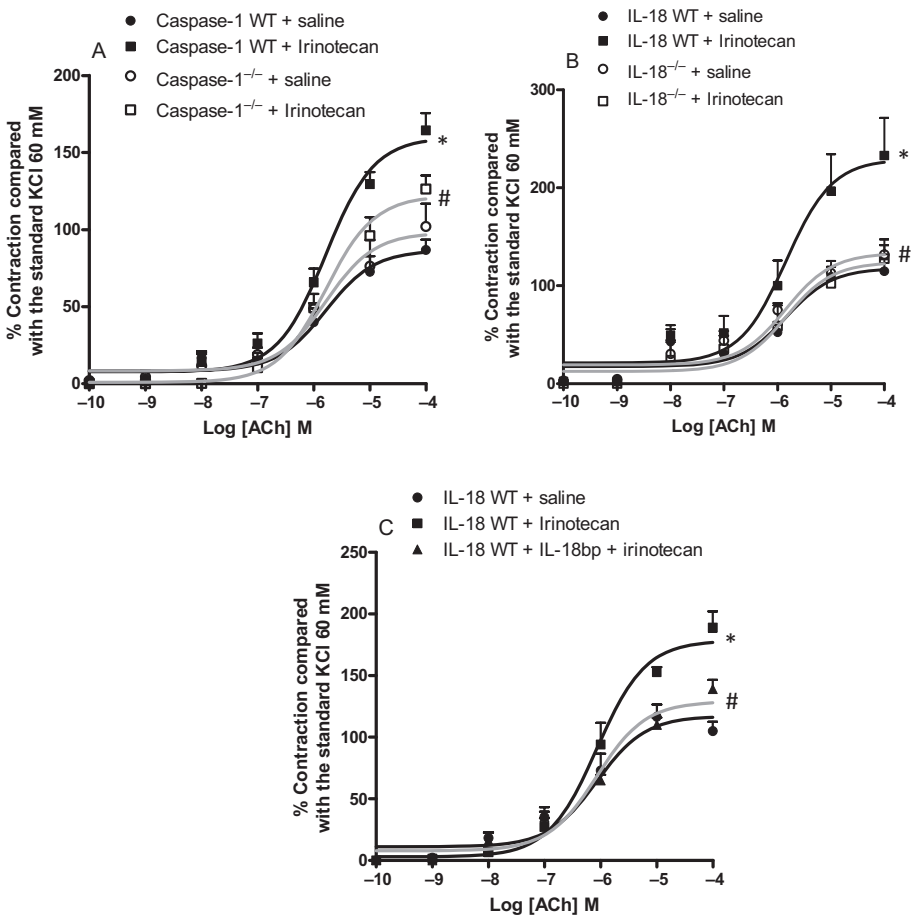

Figure 8

Irinotecan-induced effects on duodenal contractility are inhibited in caspase-1 knockout (caspase-$1^{-/-}$) , IL-18 knockout (IL-$18^{-/-}$) and WT IL-18 mice treated with IL-18bp. Concentration–response curves were constructed by adding increasing concentrations of ACh (10^{-10} to 10^{-4} M) to the bath chamber containing the isolated tissues obtained from saline- or irinotecan-treated animals. Caspase-1 knockout (panel A), IL-18 knockout (panel B), and IL-18bp-treated animals (panel C). Data shown are means ± SEM. *$P < 0.05$ versus the WT group that was injected with saline, and $^{\#}P < 0.05$ versus the irinotecan-treated WT group.

4-piperidinopiperidine portion can inhibit AChE activity *in vitro*. Expanding on these results, we demonstrated increased contractile responses of intestinal strips to ACh in the irinotecan-treated group. However, the mechanisms involved in late-onset diarrhoea remain poorly understood and are not controlled by anti-cholinergic agents. The results obtained in this study, together with the results of earlier studies (Lima-Júnior *et al.*, 2012), clearly suggest that the inflammatory reaction plays a role in intestinal hyper-contractility after systemic irinotecan administration. Nevertheless, the mechanism by which the inhibition of proinflammatory mediators blocks this phenomenon is still a matter of debate.

Some experimental studies have indicated that the activation of nicotinic receptors in inflammatory cells, such as macrophages, inhibits proinflammatory cytokine production and reduces morbidity during experimental sepsis (Borovikova *et al.*, 2000; Pavlov *et al.*, 2007). The excessive activation of such receptors by increased concentrations of ACh in the intestinal synapses during irinotecan-related intestinal mucositis may account for cholinergic receptor desensitization in inflammatory cell membranes and the increased release of inflammatory mediators. This phenomenon would lead to tissue damage, hyperresponsiveness of the gut muscle layers and the development of diarrhoea. However, this mechanism still needs to be investigated.

Severe mucositis appears to be associated with marked increases in mortality (Sonis *et al.*, 2001). Sonis *et al.* (2001) reported that oral mucositis is associated with significantly worse clinical and economic outcomes in blood and marrow transplantation, because of high-dose, myelo-ablative chemotherapy that is used for conditioning. In the Sonis study, the authors reported a 3.9-fold increase in the 100 day mortality risk in the population investigated (Sonis *et al.*, 2001). In our study in mice, a high mortality rate was associated with the irinotecan treatment. One remarkable finding from our research was the observation that both IL-18 gene deletion and IL-18bp injection markedly improved survival. In our opinion, these approaches provided optimal control of inflammatory and functional parameters, leading to higher survival rates.

It is important to mention that the inhibition of IL-18 function did not appear to interfere with irinotecan-induced

Table 2

Potency (pD_2) and maximum contractile effect (E_{max}) for the concentration–effect curves of ACh-induced mouse duodenal strip contractions

	ACh	
Group	**pD_2**	**E_{max}**
Caspase-1 WT + saline	5.83 ± 0.17	86 ± 5.5
Caspase-1 WT + irinotecan (60 mg·kg^{-1})	5.75 ± 0,10	161 ± 6.6*
Caspase-1 knockout + saline	5.90 ± 0.22	97 ± 8.0
Caspase-1 knockout + irinotecan (60 mg·kg^{-1})	5,76 ± 0.12	122 ± 6.2$^{\#}$
IL-18 WT + saline	5.79 ± 0.20	119 ± 8.8
IL-18 WT + irinotecan (60 mg·kg^{-1})	5.79 ± 0.24	232 ± 21†
IL-18 knockout + saline	6.17 ± 0.15	126 ± 6.6
IL-18 knockout + irinotecan (60 mg·kg^{-1})	5.89 ± 0.31	123 ± 14.6
IL-18 WT + saline	6.40 ± 0.16	111 ± 6.0
IL-18 WT + irinotecan (60 mg·kg^{-1})	6.00 ± 0.10	181 ± 7.4†
IL-18 WT + IL-18bp + irinotecan (60 mg·kg^{-1})	5.94 ± 0.10	132 ± 5.3$^{\$}$

*p*D2 represents the negative logarithm to base 10 of the molar concentration of ACh that produces 50% (EC_{50}) of its maximal possible effect (E_{max}). Such parameters were reported as the means ± SEM. E_{max} values for ACh-induced contractions are expressed as the % contraction compared with the standard 60 mM KCl-induced contraction followed by the SEM.
*$P < 0.001$ versus the Caspase-1 WT + saline.
$^{\#}P < 0.01$ versus the irinotecan-treated caspase-1 WT group.
$^{\dagger}P < 0.001$ versus the IL-18 WT + saline group.
$^{\$}P < 0.01$ versus the irinotecan-treated IL-18 WT group as assessed using Bonferroni's test.

cytotoxic effects. Neither IL-18bp treatment nor the genetic ablation of IL-18 or of caspase-1 prevented irinotecan-induced leukopaenia (Lima-Júnior *et al.*, 2012).

The main limitation of our study is the absence of a tumour site in this animal model. It is well recognized that the highly immunogenic cancer cells may evade immune destruction by disabling components of the immune system aimed at eliminating them (see Hanahan and Weinberg, 2011). One mechanism involved in this disabling action is the increased secretion of immunosuppressive factors and through the recruitment of inflammatory cells that are actively immunosuppressive, including regulatory T-cells (Tregs) (see Hanahan and Weinberg, 2011). Therefore, such immunoregulatory interference by could change the profile of pro-inflammatory mediators involved in the pathogenesis of cancer chemotherapy-related mucositis. We do not know whether the presence of tumour cells during the development of the experimental mucositis would change the course of this toxicity, and those aspects are still to be investigated.

In conclusion, the targeted inhibition of IL-18 attenuated irinotecan-induced intestinal mucositis in mice. As the activity of IL-18 is balanced by the presence of a high affinity, naturally occurring IL-18bp, the supplementation of endogenous IL-18bp, with exogenous IL-18bp,in order to selectively inhibit the function of IL-18 may be a promising therapeutic approach for intestinal mucositis.

Acknowledgements

We are grateful to Juliana Bertozi, Fabiola Leslie Mestriner, Ana Katia dos Santos, Rosemayre Souza Freire, Maria Silvandira Freire and Karina Felismino da Silva Santos for their technical assistance. This study was supported by CNPq (Conselho Nacional de Desenvolvimento Científico e Tecnológico), CAPES (Fundação Coordenação de Aperfeiçoamento de Pessoal de Nível Superior) and FUNCAP (Fundação Cearense de Apoio ao Desenvolvimento Científico). We also acknowledge Merck-Serono International (Geneva, Switzerland) for the supply of recombinant IL-18bp.

Author contributions

Study design: R C P Lima-Júnior; H C Freitas; G A C Brito; M M Teixeira; P J C Magalhães; M H L P Souza; F Q Cunha; R A Ribeiro. Performed the Experiments: R C P Lima-Júnior; H C Freitas; D V T Wong; C W S Wanderley; L G Nunes; L L Leite; S P Miranda. Data analysis: R C P Lima-Júnior; H C Freitas; D V T Wong; G A C Brito; M M Teixeira; P J C Magalhães; M H L P Souza; F Q Cunha; R A Ribeiro. Interpretation of the results: R C P Lima-Júnior; H C Freitas; D V T Wong; G A C Brito; M M Teixeira; P J C Magalhães; M H L P Souza; F Q Cunha; R A Ribeiro. Wrote the paper: R C P Lima-Júnior; H C Freitas; G A C Brito; M M Teixeira; P J C Magalhães; F Q Cunha; R A Ribeiro. All the authors revised and approved the paper.

Conflicts of interest

The authors indicate that they have no potential conflicts of interest.

References

Alvarez B, Radi R (2003). Peroxynitrite reactivity with amino acids and proteins. Amino Acids 25: 295–311.

Borovikova LV, Ivanova S, Zhang M, Yang H, Botchkina GI, Watkins LR *et al.* (2000). Vagus nerve stimulation attenuates the systemic inflammatory response to endotoxin. Nature 405: 458–462.

Bradley PP, Christensen RD, Rothstein G (1982). Cellular and extracellular mieloperoxidase in pyogenic inflammation. Blood 60: 618–622.

Bredt DS, Snyder SH (1989). Nitric oxide mediates glutamate-linked enhancement of cGMP levels in the cerebellum. Proc Natl Acad Sci U S A 86: 9030–9033.

Chikano S, Sawada K, Shimoyama T, Kashiwamura SI, Sugihara A, Sekikawa K *et al.* (2000). IL-18 and IL-12 induce intestinal inflammation and fatty liver in mice in an IFN-gamma dependent manner. Gut 47: 779–786.

Dinarello CA (2001). Novel targets for interleukin 18 binding protein. Ann Rheum Dis 60 (Suppl. 3): iii18–iii24.

Dinarello CA, Novick D, Kim S, Kaplanski G (2013). Interleukin-18 and IL-18 binding protein. Front Immunol 4: 1–10.

Gibson RJ, Keefe DM (2006). Cancer chemotherapy-induced diarrhoea and constipation: mechanisms of damage and prevention strategies. Support Care Cancer 14: 890–900.

Gibson RJ, Keefe DM, Lalla RV, Bateman E, Blijlevens N, Fijlstra M *et al.* (2013). Systematic review of agents for the management of gastrointestinal mucositis in cancer patients. Support Care Cancer 21: 313–326.

Hanahan D, Weinberg RA (2011). Hallmarks of cancer: the next generation. Cell 144: 646–674.

Hind D, Tappenden P, Tumur I, Eggington S, Sutcliffe P, Ryan A (2008). The use of irinotecan, oxaliplatin and raltitrexed for the treatment of advanced colorectal cancer: systematic review and economic evaluation. Health Technol Assess 12: iii–ix, xi–162.

Hsu SM, Raine L (1981). Protein A, avidin, and biotin in immunohistochemistry. J Histochem Cytochem 29: 1349–1353.

Hyatt JL, Tsurkan L, Morton CL, Yoon KJ, Harel M, Brumshtein B *et al.* (2005). Inhibition of acetylcholinesterase by the anticancer prodrug CPT-11. Chem Biol Interact 157–158: 247–252.

Ikuno N, Soda H, Watanabe M, Oka M (1995). Irinotecan (CPT-11) and characteristic mucosal changes in the mouse ileum and caecum. J Natl Cancer Inst 87: 1876–1883.

Keefe DM, Schubert MM, Elting LS, Sonis ST, Epstein JB, Raber-Durlacher JE *et al.* (2007). Updated clinical practice guidelines for the prevention and treatment of mucositis. Cancer 109: 820–831.

Kilkenny C, Browne W, Cuthill IC, Emerson M, Altman DG (2010). Animal research: reporting *in vivo* experiments: the ARRIVE guidelines. Br J Pharmacol 160: 1577–1579.

Krishna SG, Zhao W, Grazziutti ML, Sanathkumar N, Barlogie B, Anaissie EJ (2011). Incidence and risk factors for lower alimentary tract mucositis after 1529 courses of chemotherapy in a homogenous population of oncology patients: clinical and research implications. Cancer 117: 648–655.

Kurita A, Kado S, Kaneda N, Onoue M, Hashimoto S, Yokokura T (2000). Modified irinotecanhydrochloloride (CPT-11) administration schedule improves induction of delayed-onset diarrhea in rats. Cancer Chemother Pharmacol 46: 211–220.

Leach ST, Messina I, Lemberg DA, Novick D, Rubenstein M, Day AS (2008). Local and systemic interleukin-18 and interleukin-18-binding protein in children with inflammatory bowel disease. Inflamm Bowel Dis 14: 68–74.

Leitão RF, Ribeiro RA, Bellaguarda EA, Macedo FD, Silva LR, Oriá RB *et al.* (2007). Role of nitric oxide on pathogenesis of 5-fluorouracil induced experimental oral mucositis in hamster. Cancer Chemother Pharmacol 59: 603–612.

Leitão RF, Brito GA, Oriá RB, Braga-Neto MB, Bellaguarda EA, Silva JV *et al.* (2011). Role of inducible nitric oxide synthase pathway on methotrexate-induced intestinal mucositis in rodents. BMC Gastroenterol 11: 90.

Lima-Júnior RC, Figueiredo AA, Freitas HC, Melo ML, Wong DV, Leite CA *et al.* (2012). Involvement of nitric oxide on the pathogenesis of irinotecan-induced intestinal mucositis: role of cytokines on inducible nitric oxide synthase activation. Cancer Chemother Pharmacol 69: 931–942.

Livak KJ, Schmittgen TD (2001). Analysis of relative gene expression data using real-time quantitative PCR and the 2(-Delta Delta C(T)) Method. Methods 25: 402–408.

Matsunaga H, Hokari R, Ueda T, Kurihara C, Hozumi H, Higashiyama M *et al.* (2011). Physiological stress exacerbates murine colitis by enhancing proinflammatory cytokine expression that is dependent on IL-18. Am J Physiol Gastrointest Liver Physiol 301: G555–G564.

McGrath JC, Drummond GB, McLachlan EM, Kilkenny C, Wainwright CL (2010). Guidelines for reporting experiments involving animals: the ARRIVE guidelines. Br J Pharmacol 160: 1573–1576.

Melo ML, Brito GA, Soares RC, Carvalho SB, Silva JV, Soares PM *et al.* (2008). Role of cytokines (TNF-alpha, IL-1beta and KC) in the pathogenesis of CPT-11-induced intestinal mucositis in mice: effect of pentoxifylline and thalidomide. Cancer Chemother Pharmacol 61: 775–784.

Nakao T, Kurita N, Komatsu M, Yoshikawa K, Iwata T, Utusnomiya T *et al.* (2012). Irinotecan injures tight junction and causes bacterial translocation in rat. J Surg Res 173: 341–347.

Pavlov VA, Ochani M, Yang LH, Gallowitsch-Puerta M, Ochani K, Lin X *et al.* (2007). Selective alpha7-nicotinic acetylcholine receptor agonist GTS-21 improves survival in murine endotoxemia and severe sepsis. Crit Care Med 35: 1139–1144.

Peterson DE, Bensadoun RJ, Roila F (2011). Management of oral and gastrointestinal mucositis: ESMO clinical practice guidelines. Ann Oncol 22 (Suppl. 6): vi78–vi84.

Ribeiro RA, Flores CA, Cunha FQ, Ferreira SH (1991). IL-8 causes *in vivo* neutrophil migration by a cell-dependent mechanism. Immunology 73: 472–477.

Rubenstein EB, Peterson DE, Schubert M, Keefe D, McGuire D, Epstein J *et al.* (2004). Clinical practice guidelines for the prevention and treatment of cancer therapy-induced oral and gastrointestinal mucositis. Cancer 100 (9 Suppl.): 2026–2046.

Sahoo M, Ceballos-Olvera I, del Barrio L, Re F (2011). Role of the inflammasome, IL-1β, and IL-18 in bacterial infections. ScientificWorldJournal 11: 2037–2050.

Soares PM, Mota JM, Souza EP, Justino PF, Franco AX, Cunha FQ *et al*. (2013). Inflammatory intestinal damage induced by 5-fluorouracil requires IL-4. Cytokine 61: 46–49.

Sonis ST, Oster G, Fuchs H, Bellm L, Bradford WZ, Edelsberg J *et al*. (2001). Oral mucositis and the clinical and economic outcomes of hematopoietic stem-cell transplantation. J Clin Oncol 19: 2201–2205.

van de Veerdonk FL, Netea MG, Dinarello CA, Joosten LA (2011). Inflammasome activation and IL-1β and IL-18 processing during infection. Trends Immunol 32: 110–116.

Verri WA Jr, Cunha TM, Ferreira SH, Wei X, Leung BP, Fraser A *et al*. (2007). IL-15 mediates antigen-induced neutrophil migration by triggering IL-18 production. Eur J Immunol 37: 3373–3380.

Volin MV, Koch AE (2011). Interleukin-18: a mediator of inflammation and angiogenesis in rheumatoid arthritis. J Interferon Cytokine Res 31: 745–751.

Wenzl HH (2012). Diarrhea in chronic inflammatory bowel diseases. Gastroenterol Clin North Am 41: 651–675.

Wyburn KR, Chadban SJ, Kwan T, Alexander SI, Wu H (2013). Interleukin-18 binding protein therapy is protective in adriamycin nephropathy. Am J Physiol Renal Physiol 304: F68–F76.

Xynos ID, Karadima ML, Voutsas IF, Amptoulach S, Skopelitis E, Kosmas C *et al*. (2013). Chemotherapy ± cetuximab modulates peripheral immune responses in metastatic colorectal cancer. Oncology 84: 273–283.